

Hydrogen bond dynamics in water

Contact majed.chergui@epfl.ch

C. Arrell, J. Ojeda, F. van Mourik, M. Chergui

Laboratoire de Spectroscopie Ultrarapide
EPFL

Introduction

Hydrogen bonds in water are fundamental to life and a full understanding of these intermolecular bonds is necessary to explain water's unique properties. Advances in this field have been made using vibrational spectroscopic techniques mainly in the IR regime observing the progression of OH stretching modes [1,2]. A limitation of this technique however is the fundamental blindness to the intermolecular bond.

Reported here is the first application of photoelectron spectroscopy of liquids coupled to the ultrafast time resolution offered by time preserved monochromatization of high harmonics, to directly probe the intermolecular bonds. Using the time- preserved monochromatized VUV pulses from the Artemis beamline, the molecular orbitals of water were observed. The localised hydrogen bond network was broken by pumping the water sample with two quanta of vibration energy.

By measuring the binding energy of the HOMO of water, the electron forming the hydrogen bond was observed. Monitoring changes to the HOMO binding energy, the breaking and reforming of the hydrogen bond was measured as 40 fs and 80 fs respectively.

Experimental method

The time-preserving monochromator high harmonic line of the Artemis facility was used to produce a monochromatized VUV source. Using a 40 cm focal length mirror, 2 mJ of 30 fs 800 nm light was focused into a continuous flow highly localized source of atomic neon in vacuum. Through the non-linear interaction VUV photons up to 120 eV were produced, and subsequently collimated onto a gold grating with the groove direction parallel to the VUV path. In this manner a controlled number of grooves were illuminated to provide sufficient energy resolution (~ 0.8 eV) while limiting the temporal stretch of the pulse from neighbouring grooves. Previous cross-correlation measurements of the monochromatized output revealed a 30 fs FWHM VUV pulse [3]. The VUV was focused onto a liquid target with a toroidal mirror and overlapped in front of a purpose built differentially pumped time-of-flight spectrometer.

W. Okell, T. Witting, T. Siegel, Z. Diveki, S. Hutchinson, J. W. G. Tisch, J. Marangos

Attosecond Laboratory
Imperial College

The sample was excited with a 1.9 μm IR pulse generated by pumping a TOPAS with 6 mJ of the drive laser. This was temporally delayed relative to the probe VUV pulse in 10 fs steps in a 200 fs range centred at time zero. The pump pulse was temporally and spatially overlapped on the liquid target with a near collinear geometry by injecting the beam just after the toroidal mirror.

The liquid target was produced using a micro liquid jet which formed a ~ 2 mm region of laminar flow in a 20 μm diameter jet exiting from a fused silica nozzle. The liquid sample was exited from the vacuum environment approximately 1 mm below the entrance nozzle into a separate differentially pumped collection chamber. This arrangement, coupled with large cryo pumping with 30 litre capacity cold fingers maintained the interaction chamber background pressure at $\sim 5 \times 10^{-6}$ mbar.

A VUV probe energy of 38.5 eV was used and binding energy spectra of water were collected in the time-of-flight electron spectrometer. To suppress static charging of the water jet from the motion of the water over the insulating materials of the jet apparatus, 20 mM of charge carriers (NaCl) were diluted in the water.

The individual spectra were collected for 10 seconds (10,000 laser shots) before the time delay was advanced 10 fs. The entire scan (200 fs) was repeated 400 times to average fluctuations in the laser conditions over the 30 hour data collection time.

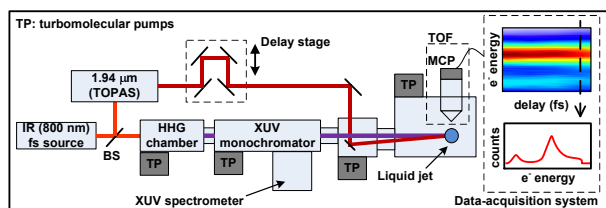


Figure 1 Schematic of the experimental setup. See experimental method section for detailed description

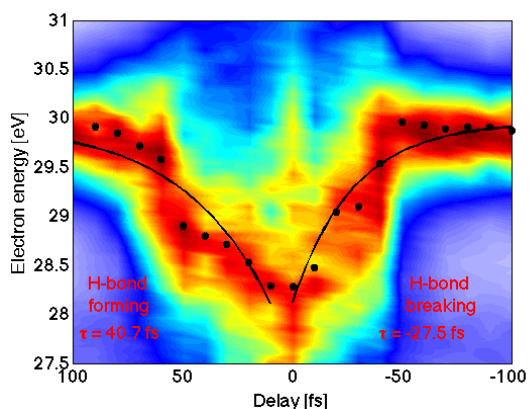


Figure 2 Centre of mass motion of the $1b_1$ liquid HOMO of water upon excitation of the combination stretch and bend mode of water. The data was collection in 10 fs steps and repeated 400 times. Right-hand side pump pulse arrives after probe pulse.

Discussion

A clear and significant shift is observed in Figure 2 of the $1b_1$ liquid HOMO. From the un-pumped level the binding energy increases by ~ 1.5 eV (note the plot in figure 2 is of electron kinetic energy) within 40 fs. This is an extremely fast motion and similar to the cross correlation of the pump and probe pulses. At 0 fs delay the distribution of the electrons is near uniform over a 3 eV bandwidth. Following time zero the centre of mass motion of the HOMO returns to the un-pumped level within 80 fs.

The observed motion of the HOMO is extremely rapid and is not explained by the slower oscillations of the excited OH stretch and bending modes of water. Significantly the time constant for the rise and fall of the HOMO binding energy is not symmetric and is approximately twice as long for the binding energy to return to the un-pumped level.

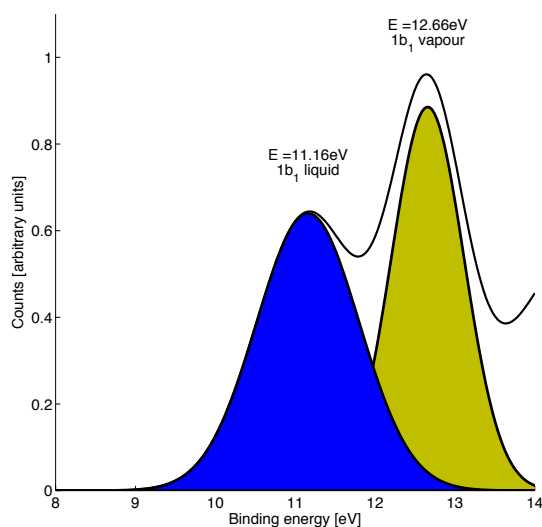


Figure 3 HOMO in liquid ($1b_1$ liquid) and gas ($1b_1$ vapour) phase water.

With all high laser field intensity measurements the pumping laser field must be accounted for in the

observed measurement. The most significant field effect in this regime is the Laser Assisted Photoelectric effect (LAPE), observed as the coherent addition or emission of pumping photons in the measured binding energy spectrum. The experimental conditions reported here are similar to [4] where a 38 eV, 30 fs probed a Pt surface pumped with 1.5 eV photons. [4] reported a convolution in the binding energy spectrum of Pt with $\pm 1,2$ pump photons, resulting in a similar spectrum observed at time zero in figure 2. However the effect in the reference was only observed at time zero, and not at other time delays. It is fair to conclude that while LAPE is present in the reported measurement, this only explains the time zero spectrum and not the 1.5 eV, unsymmetrical shift observed with 0.8 eV pumping field.

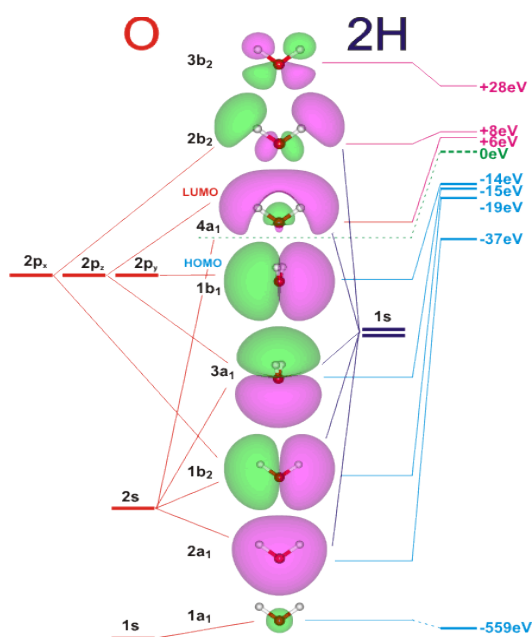


Figure 4 The electronic structure of a water molecule. The $1b_1$ HOMO is entirely oxygen centred. Figure from [5]

The large 1.5 eV binding energy shift is identical to the difference between the $1b_1$ liquid and $1b_1$ vapour binding energies, *ie* when hydrogen bonds are present and when they are not (figure 3). The source of this shift is the oxygen centred nature of the HOMO bond. The electronic structure of water is shown in figure 4 and highlights the oxygen centred HOMO bond, with no contribution from the hydrogen 1s. This is the lone pair of electrons on the oxygen atom - also the δ^- hydrogen bond acceptor in the water molecule.

When a hydrogen bond is formed the lone pair electron density is shared with the δ^+ hydrogen atom on a neighbouring water molecule, thus reducing the binding energy and giving rise to the intermolecular sensitivity of the HOMO.

The observed shift in the HOMO is a result of the rapid breaking of the localised hydrogen bond network after the absorption of two quanta of vibrational energy from the 1.9 μm pump. This ultrafast and significant energy absorption by a single molecule rapidly (~ 30 fs) shears

the hydrogen bond donor (δ^+ hydrogen atom) away from a neighbouring water molecule. Subsequently the lone pair on the neighbouring molecule forming the HOMO in water no longer share their electron density and are free from hydrogen bonding, this is the observed increase in the binding energy. After time zero, the local water molecule environment stabilises and hydrogen bonds reform. This stabilisation was measured to last ~ 80 fs, and similar in lifetime to the theoretical results of hydrogen bond flipping from librational motion reported in [6].

It is important to note reported here is the highly localised hydrogen bond breaking and reforming of the network located around an excited water molecule. This represents $\sim 20 - 30\%$ of the entire water sample affecting $40 - 60\%$ of the bonded molecules. This is different to previously reported global heating of water via IR excitation occurring on the ps timescales [7] resulting in an increase in evaporation from water. Within the time frame presented here, water molecules are not freed from the surface, or liberated from the liquid water environment. Such processes cannot occur within 80 fs.

Conclusions

With the method presented in this report, the breaking and reforming of the localised hydrogen bond network has been observed. On absorption of 2 quanta of vibrational energy, a water molecule receives a significant 'kick' removing its hydrogen atoms from the vicinity of neighbouring water molecules, breaking the hydrogen bond. After the initial rearrangement the network is restored in 80 fs.

This result allows observation of energy transfer processes taking place immediately after water excitation, and demonstrates that direct observation of intramolecular bonds allows intermolecular dynamics to be measured.

To our knowledge this is first measurement to directly observe the ultrafast hydrogen bond dynamics in water.

Acknowledgements

The authors acknowledge the mechanical support provided by the workshop of the CLF, namely S. Hook and P. Rice.

References

1. Woutersen *et al* Nature **402**, 507 – 509 (1999)
2. Fecko *et al* Science **301**, 1698 – 1702 (2003)
3. Frassetto *et al* Opt. Exp **19**, 19169 (2011)
4. Miaja-Avila *et al* PRL **97**, 112604 (2006)
5. <http://www.lsbu.ac.uk/water/h2oorb.html>
6. Laage *et al* Science **311**, 832 – 835 (2006)
7. Link *et al* Appl Phys A **96**, 117-135 (2009)

Snapshots of non-equilibrium Dirac carrier distributions in graphene

Contact Isabella.Gierz@mpsd.cfel.de

Isabella Gierz

Max Planck Institute for the Structure and Dynamics of Matter
Hamburg (Germany)

Jesse C. Petersen

Department of Physics, Clarendon Laboratory
University of Oxford
Oxford (United Kingdom)

Matteo Mitrano

Max Planck Institute for the Structure and Dynamics of Matter
Hamburg (Germany)

Cephise Cacho

Central Laser Facility
STFC Rutherford Appleton Laboratory
Harwell (United Kingdom)

Edmond Turcu

Central Laser Facility
STFC Rutherford Appleton Laboratory
Harwell (United Kingdom)

Emma Springate

Central Laser Facility
STFC Rutherford Appleton Laboratory
Harwell (United Kingdom)

Alexander Stöhr

Max Planck Institute for Solid State Research
Stuttgart (Germany)

Axel Köhler

Max Planck Institute for Solid State Research
Stuttgart (Germany)

Ulrich Starke

Max Planck Institute for Solid State Research
Stuttgart (Germany)

Andrea Cavalleri

Max Planck Institute for the Structure and Dynamics of Matter
Hamburg (Germany)
Department of Physics, Clarendon Laboratory
University of Oxford
Oxford (United Kingdom)

Introduction

Graphene, a single layer of sp^2 -bonded carbon atoms arranged in a honeycomb lattice, is one of the few ideally two-dimensional crystals available today [1]. While the in-plane σ -bonds are responsible for graphene's extreme mechanical strength, the out-of-plane π -bonds determine graphene's peculiar electronic properties. They originate from two cosine-shaped bands that cross at the Fermi-level, where they form a Dirac cone with linear instead of the conventional parabolic dispersion (see Fig. 1). Hence, charge carriers in graphene behave like massless Dirac particles, offering the possibility to investigate the predictions of relativistic quantum electrodynamics in a simple solid state system.

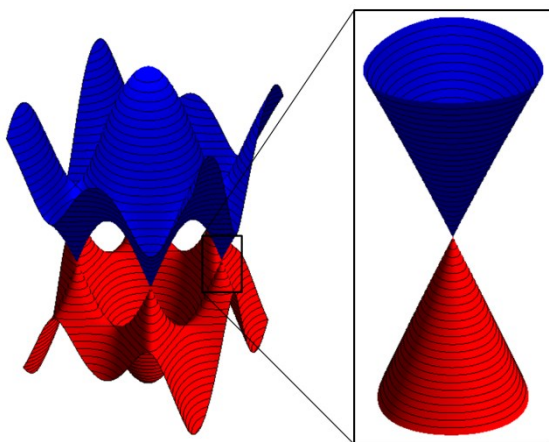


Figure 1: Graphene's electronic structure. The valence (conduction) band is shown in red (blue). Valence and conduction band touch at the Fermi level at the K-point of the hexagonal Brillouin zone forming a Dirac cone with linearly dispersing bands.

Furthermore, the extremely high mobility of the Dirac carriers has raised hopes for novel high-speed electronic devices. Unfortunately, the absence of a band gap results in low on-off ratios of graphene-based transistors severely restricting the performance of such devices.

On the other hand, the absence of a band gap leads to promising optical properties such as homogeneous broadband light absorption [2]. Furthermore, a relaxation bottleneck at the Dirac point allows for saturable absorption [3] and even light amplification [4]. Recently, it has been predicted that the absorption of a single photon might create several electron-hole pairs by impact ionization [5], an effect that would increase the efficiency of graphene-based solar cells considerably.

We set out to investigate graphene's potential for optoelectronics with time- and angle-resolved photoemission spectroscopy (ARPES), a technique that gives direct access to the transient occupation of the Dirac cone over a broad energy range in momentum space [6].

Sample preparation

Epitaxial growth of graphene on silicon carbide (SiC) is the method of choice to obtain homogeneous, large-area graphene monolayers on a semiconducting substrate suitable for spectroscopic characterization with ARPES. For the present investigation we used lightly hole-doped graphene monolayers on hydrogen-terminated SiC(0001) that have been grown as described in [7].

The static band structure in the vicinity of the K-point (see Fig. 2a) is shown in Fig. 2b. For measurements perpendicular to the Γ K-direction, extrapolation of the bands based on a tight-binding model (dashed lines) [8] shows that the graphene layer is hole-doped, with the Dirac point ~ 200 meV above the static chemical potential μ_c . For measurements along Γ K, only one of the two π -bands is visible due to photoemission matrix element effects [9].

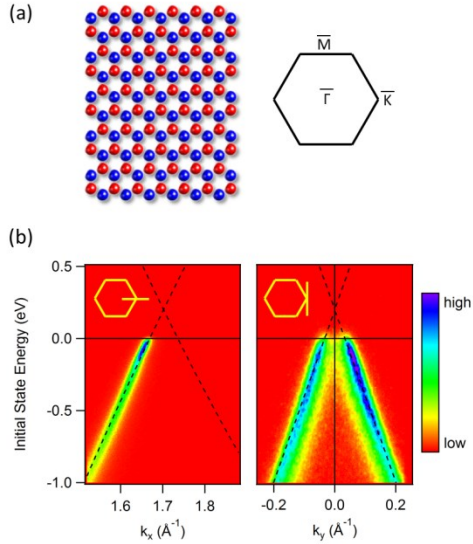


Figure 2: (a) Honeycomb lattice with hexagonal Brillouin zone. The two triangular sublattices are shown in red and blue, respectively. (b) Equilibrium band structure measured with linearly polarized synchrotron radiation ($h\nu = 30$ eV, left) and He II radiation ($h\nu = 41$ eV, right). The color scale is linear with violet (red) corresponding to high (low) photocurrent. The inset shows the cut through the Brillouin zone along which the photoemission data has been measured. Dashed black lines represent the dispersion obtained from a tight-binding model [8].

Time-resolved ARPES

ARPES is based on the photoelectric effect where the sample is illuminated with ultra-violet light and photoelectrons are ejected. These photoelectrons are sorted with respect to their kinetic energy and emission angle in a hemispherical analyzer and counted on a two-dimensional detector. The resulting two-dimensional image directly reveals a snapshot of the band structure within a certain momentum and energy range.

Time-resolved ARPES measurements were performed at the materials science end station at Artemis, using synchronized near-infrared (NIR) and extreme ultra-violet (EUV) photons as pump and probe pulses, respectively. The facility is equipped with a 1 kHz Ti:Sapphire laser system that delivers pulses with a central wavelength of 790 nm and a nominal pulse duration of 30 femtoseconds. NIR photons at $h\nu_{\text{pump}} = 950$ meV are generated via optical parametric amplification. EUV photons in the range from 20 to 40 eV are obtained via high harmonics generation in an Argon gas jet. For the present experiment a photon energy of $h\nu_{\text{probe}} = 31.5$ eV has been chosen, enabling access to electrons emitted at the K-point of the two-dimensional graphene Brillouin zone (see Fig. 2a). The energy resolution for the present experiment was 130 meV, mainly limited by the EUV pulse duration.

Figure 3 shows snapshots of the Dirac cone for different time delays after excitation of the sample at $h\nu_{\text{pump}} = 950$ meV with a fluence of 4.6 mJ/cm², transferring electrons from the valence into the conduction band. During such interband excitation, a non-thermal distribution of excited electron-hole pairs is generated at the earliest time delays, relaxing into a quasi-equilibrium state with a temperature higher than that of the lattice. Importantly, depending on the relative strength of interband versus intraband scattering, a single Fermi-Dirac distribution, or two distinct distributions for valence and conduction band are attained. Only the latter scenario would make light amplification possible.

Within the time resolution of our measurement we did not resolve non-thermal energy distributions for the Dirac electrons, indicating very efficient thermalization. Rather, we observed instantaneous broadening of the carrier distribution through the Dirac point (Fig. 3, middle panel) and subsequent relaxation within ~ 1 picosecond (Fig. 3, right panel).

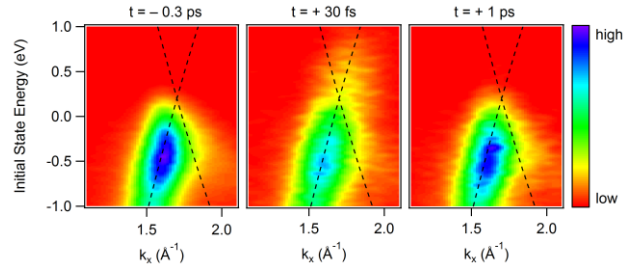


Figure 3: Snapshots of the band structure (smoothed) for excitation at $h\nu_{\text{pump}} = 950$ meV with a fluence of $F = 4.6$ mJ/cm² and a probe photon energy of $h\nu_{\text{probe}} = 31.5$ eV. The measurements were done along the ΓK -direction (inset). Dashed black lines represent the dispersion obtained from a tight-binding model [8].

Population inversion

A quantitative analysis of these dynamics is shown in Fig. 4. In panel (a) we display energy distribution curves (EDCs) as a function of pump-probe delay that have been integrated at each time delay over the momentum range depicted in Fig. 3. Zero delay corresponds to the maximum pump-probe signal. In Fig. 4b we show EDCs for selected time delays. The energy dependence of the EDCs for negative time delays (blue data points) as well as for delays $t > 130$ femtoseconds (green data points) is well fitted by the Fermi-Dirac distribution (continuous black lines). In contrast, the carrier distributions measured immediately after excitation (red data points) are best fitted by two separate Fermi-Dirac distributions for valence and conduction band, indicating population inversion [4].

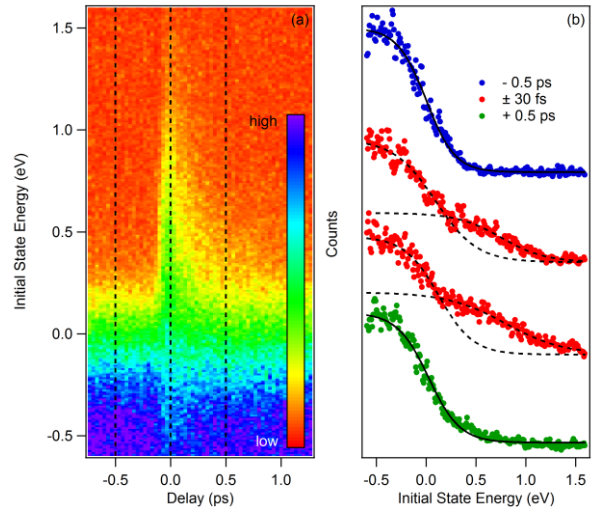


Figure 4: (a) Momentum-integrated energy distribution curves (EDCs) as a function of delay. (b) EDCs for three selected delays extracted along the dashed lines in (a) together with Fermi-Dirac distribution fits.

The two distributions merge within ~ 130 femtoseconds, and a single Fermi-Dirac distribution is attained, promoted by scattering of charge carriers across the Dirac point. As amplification is only possible for the given time window, our measurement sets a quantitative boundary to be used as a benchmark for any laser design.

Carrier multiplication

Our measurements also provide a direct assessment of the possibility of carrier multiplication in graphene [5]. Figure 5 displays the time-dependent evolution of the pump-probe signal after direct interband excitation. Specifically, Fig. 5a shows the pump-induced changes of the photocurrent as a function of energy and time delay. Blue (red) corresponds to a gain (loss) in photocurrent with respect to negative time delays. In Fig. 5b, the time derivative of the pump-probe signal of panel (a) is displayed, directly revealing the electron-hole pair generation/recombination rates. The rate above the Fermi level

is positive only for a few tens of femtoseconds. We conclude that electron-hole pairs are generated only while the pump pulse is present, whereas no spontaneous carrier multiplication is found.

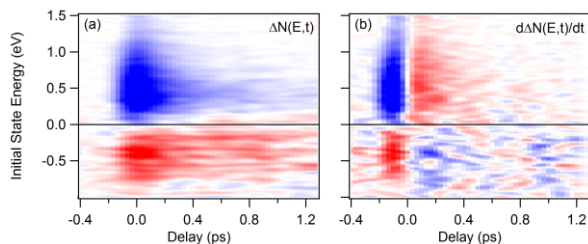


Figure 5: (a) Pump-induced changes of the photocurrent reveal the change in occupation of the Dirac cone. Blue (red) corresponds to a gain (loss) in photocurrent with respect to negative time delays. (b) Time-derivative of panel (a).

The absence of carrier multiplication and the short lifetime of electron-hole pairs discussed above raise serious doubts about the suitability of graphene for efficient light harvesting, at least in the present excitation regime. One may speculate that more favorable conditions for carrier multiplication may be met for negligible doping of the graphene layer, smaller pump fluences and higher excitation energies [5].

Conclusions

In summary, we have used time- and angle-resolved photoemission in the EUV as a tool to critically assess the potential of graphene for optoelectronic applications. We show that population inversion occurs immediately after interband excitation. By directly measuring the band occupancy $N(E,t)$ at all energies and times, we have made a quantitative evaluation of the relevance of carrier multiplication.

Acknowledgements

We thank Martin Eckstein and Franz Kärtner for fruitful discussions. Stiven Forti, Camilla Coletti and Konstantin V. Emtsev helped with the static ARPES measurements, partially supported by the German Research Foundation (DFG) within the priority program “graphene” SPP 1459 (Sta 315/8-1). Phil Rice, Richard Chapman and Natércia Rodrigues are acknowledged for technical support during the Artemis beamtime that was funded by Laserlab Europe.

References

1. A. K. Geim and K. Novoselov, *Nature Materials* **6**, 183 (2007)
2. R. R. Nair et al., *Science* **320**, 1308 (2008)
3. Q. Bao et al., *Adv. Funct. Mater.* **19**, 3077 (2009); Z. Sun et al., *ACS Nano* **4**, 803 (2010)
4. T. Li et al., *Phys. Rev. Lett.* **108**, 167401 (2012)
5. T. Winzer et al., *Nano Lett.* **10**, 4839 (2010); T. Winzer and E. Malić, *Phys. Rev. B* **85**, 241404(R) (2012)
6. I. Gierz et al., arXiv:1304.1389 (2013)
7. C. Riedl et al., *Phys. Rev. Lett.* **103**, 246804 (2009)
8. A. Bostwick et al., *Nature Physics* **3**, 36 (2007)
9. E. L. Shirley et al., *Phys. Rev. B* **51**, 13614 (1995)

Watching Hot Electrons Decay on the Dirac Cone in Graphene

Contact jens.johannsen@epfl.ch and ulstrup@phys.au.dk

Jens Christian Johannsen & Marco Grioni

École Polytechnique Fédérale de Lausanne (EPFL), Lausanne, Switzerland

Federico Cliento, Alberto Crepaldi, Michele Zacchigna & Fulvio Parmigiani

University of Trieste and Sincrotrone Trieste, Trieste, Italy

Felix Fromm, Christian Raidel & Thomas Seyller

Technische Universität Chemnitz, Chemnitz, Germany

Søren Ulstrup & Philip Hofmann

Aarhus University, Aarhus, Denmark

Cephise Cacho, Edmund Turcu & Emma Springate

Central Laser Facility, STFC Rutherford Appleton Laboratory, Didcot, United Kingdom

Introduction

Graphene is thought to be one of the most promising materials for future photonics devices. Its perhaps most peculiar property is that its charge carriers behave as if they were mass less relativistic particles with an energy that is linear in momentum [1]. In consequence, the graphene layer displays a wavelength-independent optical absorption of 2.3 % despite being only one-atom thick. In conjunction with an ultrahigh carrier mobility, this property renders graphene very interesting for novel light-harvesting applications [2]. A detailed understanding of the out-of-equilibrium dynamics of the hot carrier distribution before it reaches a thermal equilibrium with the lattice is an essential requirement for making progress towards this end. Owing to the unique combination of a XUV beamline and an angle resolved photoemission (ARPES) end-station at the Artemis facility, we were able to perform the first direct time resolved study of the dynamics in the Dirac cone of graphene, permitting us to address several outstanding questions on this important material.

Movies of Hot Electrons using TR-ARPES

At the Artemis facility it is possible to ‘shoot movies’ of the out-of-equilibrium electronic structure of a condensed matter system. As for every good action movie it is important to catch the main actors at play with the highest resolution and in the best light. For a condensed matter system the actors are the quasiparticle excitations of the electronic structure.

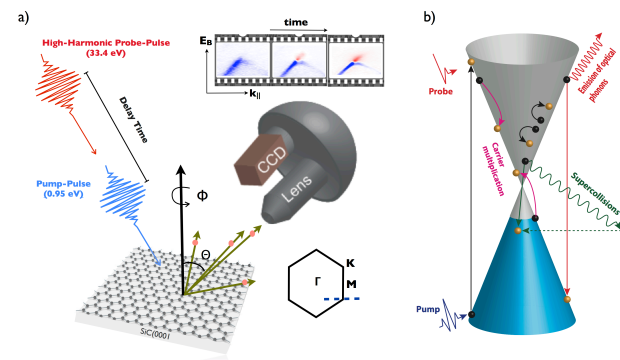


Fig. 1: **a)** Sketch of the time resolved ARPES experiment. An infrared pulse excites the electrons in the graphene layer while a delayed XUV pulse emits the photoelectrons whose energy and emission angle is mapped onto the 2D detector in the hemispherical energy analyser. Using simple kinematic relations the image is easily converted into an energy-momentum map. Varying the delay time allow the scientists to explore the temporal evolution of the electronic structure. **b)** Illustration of the dominant decay mechanisms taking place in the Dirac spectrum of graphene after exciting with a pump pulse.

Owing to the combination of a widely tunable laser source with ultrafast short-pulsed XUV (10 to 100 eV) radiation produced through high harmonic generation, and a high resolution electron spectrometer operating in angle-resolving imaging mode, the Artemis facility provides the scientific filmmakers with a unique opportunity to closely follow the temporal evolution of excitations taking place even at high-momentum electron states.

The theme for our movie is the response of the electronic system in slightly hole doped graphene upon photoexcitation with a photon of sufficient energy to induce direct interband transitions. Our graphene layer is situated on an insulating SiC substrate whose top-most layer is passivated with hydrogen in order to eliminate any structural influence of the interface on the pristine electronic properties of the graphene layer [3].

Supercollisions on the Dirac Cone

By following the response in the spectral function with femtosecond time resolution, we have direct access to the statistical distribution of hot electrons. Our quantitative analysis method permits us to conclude that the thermalisation to a hot Fermi-Dirac distribution having a temperature higher than 2000 K takes place on an ultrafast time scale shorter than our time resolution (60 fs). As a result, we can determine the exact value of the temperature of the hot electrons immediately upon excitation and follow its subsequent temporal evolution.

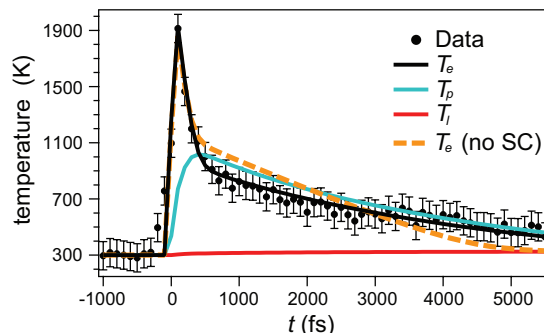


Fig. 2: Electronic temperature $T_e(t)$ as a function of delay time. Solid black line (dashed amber line) shows the converged fit to the data with (and without) the supercollision term implemented in our three-temperature model.

To quantitatively analyze the relaxation of the hot electrons, we employ a phenomenological three-temperature model. The optical phonon energies in graphene are unusually high ($\Omega = 200$ meV). As a result, the optical phonons mediate cooling for only

very hot electrons. For hot electrons below the energy Ω , the emission of acoustic modes is the only efficient cooling channel. The small size of the Fermi surface together with the requirement of momentum conservation in the scattering with the acoustic phonons imposes a severe bottleneck on the cooling. It has been predicted that disorder inherent to the graphene layer can effectively relieve this bottleneck by removing the momentum conservation constraint. This alternative cooling pathway is called *supercollision cooling* and involves three-body collision events between electron, phonons and impurities [4-6]. Our three-temperature model describes the interaction of the hot electrons with a high-energy (200 meV) optical phonon mode and with the entire thermalised distribution of acoustic modes via the supercollision mechanism.

The most striking result to emerge from our model fit to the extracted temperature data is that the supercollision mechanism does indeed seem to dominate the cooling of carriers in our low-doped and weakly disordered graphene system. Furthermore, we can extract values for the electron-phonon interaction strengths, thereby providing inputs to the current controversy on this issue.

Hot Carrier Multiplication in Graphene

One of the main objectives vigorously pursued in the fields of photonics and optoelectronics concerns identifying materials in which carrier multiplication (CM), i.e. the process by which multiple electron-hole pairs are generated upon the absorption of a single photon, can occur. Given graphene's decisive advantages for applications in future optoelectronic devices, it would be highly desirable if evidence for hot carrier multiplication could be provided also for this system. Theory strongly suggests that the thermalisation of the hot electrons in graphene under certain experimental conditions can indeed be accompanied by a carrier multiplication [7-8].

Given the fact that the system follows a Fermi-Dirac distribution with a well-defined temperature, we are able to quantify the CM in our graphene system. We find that CM in our system merely reaches a value of ~ 0.5 , i.e. it does not reach values above unity that would imply the generation of more than one electron-hole pair per absorbed photon. This result is in good agreement with what is predicted for our experimental conditions and provides experimental support for the idea that a significant CM is indeed possible in graphene, especially for higher photon energies and lower fluence.

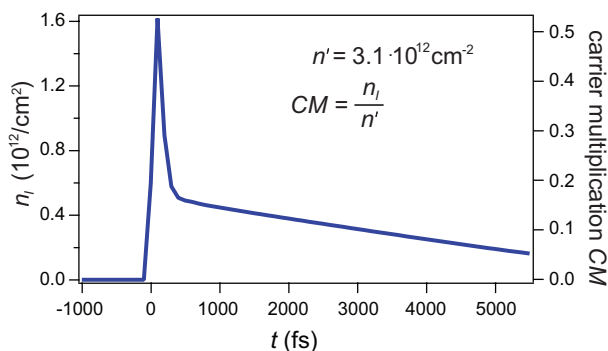


Fig. 3: Photoinduced carrier density n_i and carrier multiplication (CM) calculated from the fitted electronic temperature.

For more details concerning this work see Ref. [9].

Conclusions

Using the state-of-the-art femtosecond resolved setup at the Artemis facility, we performed the first ARPES study of the ultrafast electron dynamics in graphene. Having direct access to the energy - and momentum resolved occupation of electrons and holes we addressed the role of supercollisions in the relaxation of the hot electrons and made a quantitative evaluation of the relevance of carrier multiplication. The possibility of a significant carrier multiplication in graphene holds great promises for future high-efficiency graphene-based light-harvesting devices.

Acknowledgements

We thank Lars Bojer Madsen (Aarhus University), Torben Winzer and Ermin Malić (Technical University of Berlin) and Barbara Ressel (University of Nova Gorica) for helpful discussions. We are grateful to Phil Rice, Natercia Rodrigues, and Richard Chapman (CLF) for technical support during the beam time at the Artemis Facility.

References

1. A.H.Castro Neto *et al.*; Rev. Mod. Phys. **81**, 109-162 (2009)
2. F. Bonaccorso *et al.*; Nat. Photonics **4**, 611 (2010)
3. C. Riedl *et al.*; Phys. Rev. Lett. **103**, 246804 (2009)
4. J.W. Song *et al.*; Phys. Rev. Lett. **109**, 106602 (2012)
5. M.W. Graham *et al.*; Nat. Phys. **9**, 103 (2013)
6. Betz *et al.*; Nat. Phys. **9**, 109 (2013)
7. T. Winzer *et al.*; Nano Lett. **10**, 4839 (2010)
8. T. Winzer *et al.*; Phys. Rev. B **85**, 241404 (2012)
9. Johannsen & Ulstrup *et al.*; Phys. Rev. Lett. **111**, 027403 (2013)

UV pump XUV probe photoelectron spectroscopy

Contact r.s.minns@soton.ac.uk

R. Chapman and R.S. Minns

Chemistry, University of Southampton,
Highfield Campus, Southampton, SO17 1BJ

R. Spesyvtsev, O.M. Kirkby and H.H. Fielding

Department of Chemistry, University College London, 20
Gordon Street, London WC1H 0AJ

G. Roberts and V.G. Stavros

Department of Chemistry, University of Warwick
Coventry, CV4 7AL

S. Weber, F. Frank and J.P. Marangos

Department of Physics, Imperial College London
London, SW7 2 AZ

D.M.P. Holland

Photon Science Department, STFC Daresbury Laboratory,
Warrington WA4 4AD

I.C.E. Turcu, C.E. Caucho and E. Springate

Central Laser Facility, STFC Rutherford Appleton Laboratory
Didcot, UK

Introduction

Time resolved photoelectron spectroscopy (TRPES) has proved itself as a key technique in the study of photoinduced molecular dynamics [1]. The basic concept of TRPES is that a chemical event is triggered with an ultrashort laser pulse (pump) and the molecular system being investigated is subsequently ionised by a second, time-delayed, laser pulse (probe) at a series of different delays after excitation. The energies and angular distributions of the outgoing electrons are measured and the dynamics of the system are inferred from changes in the measured photoelectron image. One of the main reasons for its ubiquity is that all states can be ionized, in principle, meaning that it should be possible to measure the entire reaction coordinate using this method. Despite this, in most cases it has not been possible to ionise the entire reaction coordinate due to some reactive intermediates and products having large ionization limits and/or poor overlap with the ionization continuum. This leads to significant “blind spots” in the reaction mechanism, where no information about the system is obtainable. The limiting factor has been the wavelength range over which conventional femtosecond lasers can work.

Recent developments in the generation of high energy femtosecond light pulses are set to revolutionize atomic, molecular and optical science. One lab-based route to femtosecond duration pulses of VUV to soft X-ray radiation is high harmonic generation (HHG). In HHG, a strong laser pulse induces the ionisation, acceleration and subsequent re-collision of an electron from a noble gas leading to the emission of a highly energetic photon on a femtosecond or even sub-femtosecond timescale [2]. The femtosecond duration of the light source lends itself to the grand challenge of understanding chemical reactivity and molecular dynamics which occur on this fundamental timescale. Using the high energy photons produced *via* HHG as the probe in a TRPES experiment is one solution to the problem of limited energy range of conventional laser sources. The experiments described below outline the recent developments at Artemis towards using XUV light from a HHG source for time-resolved photoelectron imaging experiments.

Experimental

The experiments rely heavily on the stability and repeatability of the high harmonic generation source and monochromator. During a previous experimental run, it was noted that movement of the monochromator shifted the VUV beam spatially, meaning overlap between the pump and probe pulses could not be maintained. With no way of measuring the offset, it proved impossible to obtain a pump-probe signal. Since then, we have installed an imaging system which can image the pump and probe beams at the interaction region. With a reliable measure of the XUV and UV beam overlap, it has now been

possible to obtain pump-probe photoionization signals in helium and aniline. In both cases the pump and probe beams were generated from the output of the Red Dragon laser system (10 mJ, 40 fs, 1 kHz, 780 nm). Approximately 1 mJ of the output was focused into a gas jet of Argon producing a series of harmonics, which were separated and selected in the pulse length preserving monochromator. After the monochromator, the harmonic flux was measured to be on the order of 10^6 photons per harmonic per second. The harmonic beam served as the pump beam in the experiments with helium and as the probe beam in the experiments with aniline. The second beam was generated *via* the high energy OPA (TOPAS); 8 mJ of the Red Dragon output was used to pump the TOPAS, which after sum-frequency generation and second harmonic generation of the signal produced approximately 10 μ J of UV light around 255 nm. The two beams were focused into the velocity map imaging spectrometer where they crossed at a small angle ($\sim 1^\circ$) in the center of the interaction region.

Results

Helium

In order to demonstrate that we had achieved spatial and temporal overlap of the pump and probe pulses, we looked initially at the $1+1'$ ionisation of helium. By tuning the monochromator to the 15th harmonic (52 nm) we hit a resonance with the $1s4p$ state in He. With the absorption of a further UV photon at 255 nm, we could then ionize to He^+ . In order to be in resonance we had to blue shift the harmonic peak slightly, but once this had been achieved we could measure a clear step in the ionization signal as we varied the delay

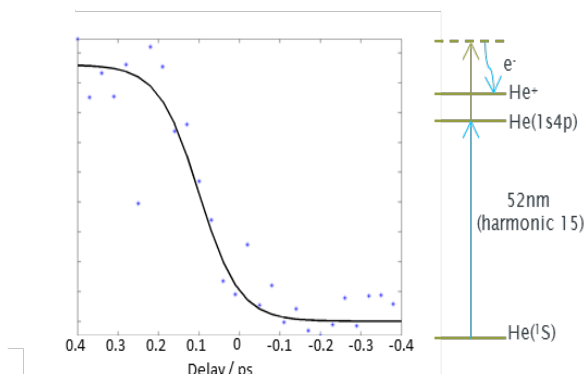


Figure 1: Change in He^+ ion signal as a function of pump-probe delay. Positive delay means that the VUV pulse is arriving first (left). The signal is a consequence of resonant excitation of the He $1s4p$ state with the 15th harmonic, followed by ionisation with the UV pulse at 255 nm (right) generated by the TOPAS

between the pump and probe beams (figure 1). The signal is extremely long lived lasting for several nanoseconds.

Aniline

Having confirmed that temporal and spatial overlap had been achieved, we moved on to the main molecule of study - aniline. Aniline ($C_6H_5NH_2$) is the simplest aromatic amine and is, therefore, a model for more complex aromatic amines such as the DNA bases adenine, cytosine and guanine. The UV spectroscopy of aniline is well known; the absorption spectrum is dominated by two strong absorption bands that correspond to $^1\pi\pi^*$ transitions from S_0 to optically bright states centered around 290 and 235 nm.

A number of recent experiments have employed various UV pump UV probe femtosecond time-resolved spectroscopy measurements to monitor the ultrafast decay of aniline following UV excitation. The experiments highlight the energy flow between the various optically bright and dark states and provide timescales for some of these energy transfer processes [3-7]; however, none of the experiments can follow the entire reaction co-ordinate back to the ground-state or explicitly link final products with a particular reaction pathway. To obtain this information, we need to monitor the entire reaction coordinate from the initially prepared electronically excited state, along the excited state potential energy surface to all products, including the ground-state and any photodissociation or photoisomerisation products. This requires a VUV probe.

Experimentally, there are many disadvantages of working with aniline compared to helium. First, it is a liquid which makes sample delivery more difficult and, due to the complex nature of the molecule, it has more diffuse photoelectron bands. This makes the pump-probe signal much less obvious than in the case of helium and as a result required us to subtract pump-only and probe-only background signals. In order to provide a proof of principle measurement, we collected images with the pump arriving 10 ps before the probe and complementary images with the probe arriving 10 ps before the pump; the difference between our pump-probe signal and these images was a genuine pump-probe signal. These images were collected over the course of 2 hours. Each image is a composite of many images collected for 30 s each. After each frame, the translation stage is moved to the alternate position where a new image is collected for 30 s. This repeated movement removes problems associated with long term drifts in power or pointing that could otherwise

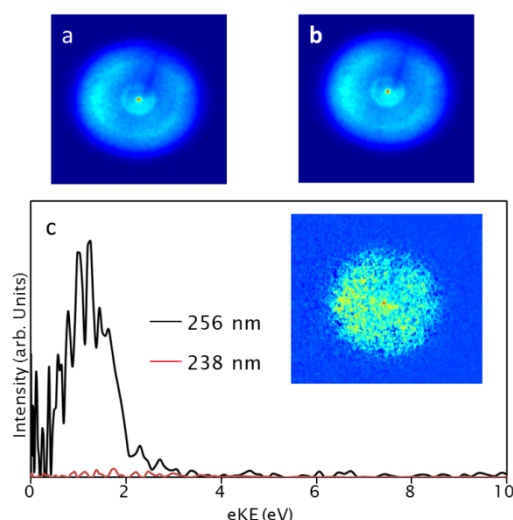


Figure 2: a) VUV + UV signal with UV coming 10 ps before the VUV. b) VUV + UV signal with VUV coming 10 ps before the VUV. c) inset. Difference between a) and b) showing the pump probe component of the signal. Main. Photoelectron spectrum of the pump probe signal at two different pump wavelengths.

lead to artifact in the subtracted image. This process was repeated for two different pump wavelengths and the results are shown in figure 2.

At a pump wavelength of 256 nm a clear difference between the two delay positions is observed. The photoelectron signal does not correlate with any of the bands associated with either pump or probe individually and therefore does not appear to be due to a bad background subtraction. When we perform the same process at a different wavelength, 236 nm, no such feature is present, again suggesting the background subtraction process is working. The signal obtained with the 256 nm pump produces a broad photoelectron feature with a maximum energy of approximately 2 eV. This cut-off matches what would be expected for ionization of the anilino radical (C_6H_5NH) dissociation product of aniline, although assignment cannot be confidently made without significantly more data.

Summary

VUV-pump-UV-probe ion signal in helium (figure 1) and UV-pump-VUV-probe photoelectron images in aniline (figure 2) have been measured. The experiments demonstrate the feasibility of performing time-resolved photoelectron spectroscopy experiments with a high harmonic generation based probe.

Acknowledgements

RSM thank the Royal Society for a University Research Fellowship and a research grant (RG110310). VGS thanks the Royal Society for a University Research Fellowship. HHF and RS are grateful to the European Marie Curie Initial Training Network Grant No. CA-ITN-214962-FASTQUAST for a studentship (RS).

References

1. Stolow A. Underwood J.G. *Adv. Chem. Phys.* **139** 497 (2008)
2. Corkum P.B. *Phys. Rev. Lett.* **71** 1994 (1993)
3. Roberts G.M. *et al* *J. Am. Chem. Soc.* **124** 13578 (2012)
4. Spesyvtsev R. *et al* *Phys. Chem. Chem. Phys.* **14** 9942 (2012)
5. King, Oliver and Ashfold, *J. Chem. Phys.*, **132**, 214307 (2010)
6. Satzger, Townsend, Zgierski, Patchkovskii, Ullrich and Stolow, *PNAS*, **103**, 10196 (2006)
7. Montero, Conde, Ovejas, Martinez, Castano and Longarte, *J. Chem. Phys.*, **135**, 154308 (2011)

Two-colour HHG spectroscopy and wavelength dependence of HHG in aligned molecules

Contact rtorres@clpu.es

Felicity McGrath, Chris Hutchison, Thomas Siegel, and
Jon P. Marangos

Blackett Laboratory, Imperial College London
Prince Consort Road, SW7 2BW London, UK

Cephise Cacho, Edmond Turcu, and Emma Springate

Central Laser Facility, Rutherford Appleton Laboratory, STFC
Chilton, Didcot, Oxon, OX11 0QX

Íñigo J. Sola

Grupo de Investigación en Óptica Extrema, Universidad de
Salamanca
Plaza de la Merced s/n, 37008 Salamanca, Spain

Ricardo Torres

Centro de Láseres Pulsados
Parque Científico de la Universidad de Salamanca, 37185,
Villamayor, Salamanca, Spain

Introduction

High harmonic generation (HHG) with strong laser fields has proven a unique tool for studying molecular structure and dynamics. The potential of HHG for probing molecules lies in the fact that the recolliding electrons that cause HHG can transfer information about the instantaneous structure of the molecule to the spectrum [1,2]. The molecular structure measured by HHG is almost frozen in time, allowing it to register the dynamics of molecules with a time resolution of a few attoseconds [3].

The revolutionary potential of HHG spectroscopy to track molecular dynamics has spurred its development during the last few years. Nevertheless, this development has been marked by obstacles. Experimentally, one of the main difficulties of HHG spectroscopy is to produce a large enough harmonic spectrum to obtain sufficient structural and dynamical information of the molecule. The maximum energy of the photons emitted by HHG is given by $E_{\max} = I_p + 3.2U_p$, where I_p is the ionisation potential of the molecule and U_p is the ponderomotive energy of the electrons in the laser field. The ponderomotive energy scales as $U_p \sim I\lambda^2$, where I is the laser intensity and λ is the wavelength. Using a laser at 800 nm, an intensity of almost 3×10^{14} W/cm² is required to obtain a harmonic cut-off of 60 eV, however, at this intensity most molecular gases suffer an excess of ionisation which impairs the propagation of the harmonics.

Several approaches have been attempted to extend the techniques of HHG spectroscopy towards organic molecules by reducing the effects of an excessive ionisation in the medium: Using ultrashort pulses ($\tau \sim 15$ fs) [4,5]; generating harmonics with a mid-IR (1300 nm) laser source [6,7]; and generating harmonics with few-cycle pulses in the mid-IR [8].

As can be seen from the above definition of U_p , the harmonic cut-off can be extended by increasing the laser wavelength whilst maintaining a relatively low intensity [9]. However, due to dispersion of the electronic wavepacket in the continuum, the intensity of the harmonics decreases rapidly with increasing laser wavelength, at a rate approximately proportional to λ^{-6} [10]. A high repetition rate (~ 1 kHz) is mandatory in order to get a good signal-to-noise ratio in the measurements, but it was thought that the steep fall-off in conversion efficiency would impede the generation of harmonics from wavelengths much longer than 1600 nm.

It has been found theoretically that a suitable combination of multi-colour fields could produce harmonic spectra with the high cut-off energy defined by the longer wavelength and an efficiency close to that achieved by the short wavelength pulse alone [11]. A simplified version of this idea was experimentally

demonstrated using a sum of two un-related frequencies [12]. In this way the enhancement of the harmonic signal was independent of the phase difference between the fields, simplifying the setup whilst offering very robust enhancement.

Here we have tested the limits of HHG in aligned molecules by increasing the wavelength of a single-colour driving field deeper into the mid-IR. Also, we have applied a two-colour scheme in order to enhance the signal of extended harmonic spectra in aligned molecules.

Experimental setup

The experiment was configured as a three-arm interferometer (Fig. 1). Two independently compressed beams of the Artemis laser were used. The output of compressor 1 (~ 8 mJ) was used to pump an Optical Parametric Amplifier (HE-TOPAS) to produce pulses of wavelengths between 1.6 and 2.0 μm (idler), ~ 30 fs duration, and ~ 500 μJ of energy. The output of compressor 2 was split in two by a 50/50 beam splitter and each sent through a motorised delay stage with an accuracy better than ± 5 fs. One of the pulses, overlapped with the mid-IR one could be used to enhance the harmonics, whereas the other, synchronised with the other two at a variable delay was used to align the molecules. A half-wave plate in the aligning beam was employed to control the angle of molecular alignment. The three beams were combined by means of a dichroic mirror and focused onto a gas jet inside the chamber by a silver coated spherical mirror of 30 cm focal length. The gas jet was produced by expansion of ~ 1 atm of gas through an open nozzle of 100 μm diameter in order to achieve the rotational cooling necessary for an efficient alignment. The harmonics produced in the interaction of the laser with the gas jet were analysed with a flat-field XUV spectrometer.

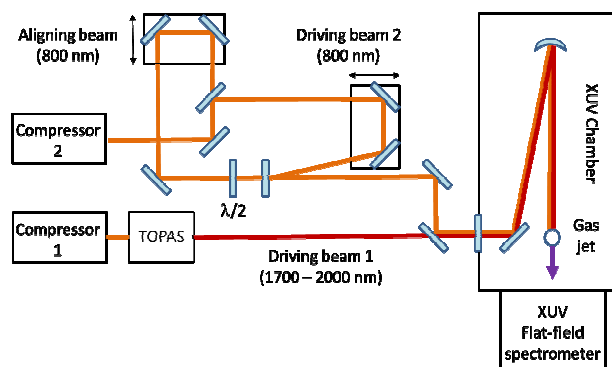


Figure 1. Scheme of the optical layout used in the experiment.

Results

The molecules we investigated were N_2 ($I_p = 15.6$ eV), CO_2 ($I_p = 13.8$ eV), and ethylene ($I_p = 10.5$ eV). The two-colour field did not enhance the signal of the higher harmonic orders as we were expecting. Instead it produced a remarkable increase only on the lower harmonics (Fig. 2a). The spectra obtained with a single-colour field at 1700 nm turned out to be good enough for HHG spectroscopy, producing clear cut-offs up to 100 eV (Fig. 2c). Furthermore, the signal ratios between spectra of aligned and nonaligned molecules showed similar characteristics for the two-colour and single-colour fields (Figs. 2b and 2d).

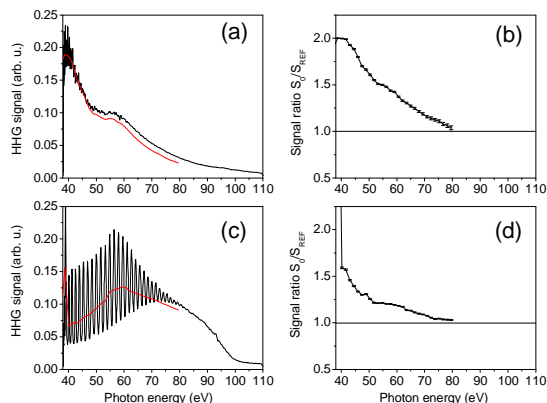


Figure 2. (a) HHG spectrum of aligned N_2 using a two-colour field of 1700 nm and 800 nm. The red line is the smoothed spectrum (integrated peaks with subtracted background). (b) Ratio between smoothed two-colour HHG spectra of aligned (parallel to the driving field) and non-aligned N_2 . (c, d), same as (a,b) for a single-colour 800 nm field.

Having realised that the 1700 nm beam generated an intense harmonic spectrum by itself we obtained a series of harmonic spectra in CO_2 and ethylene with increasing wavelengths in the driving field (Figs. 3 and 4).

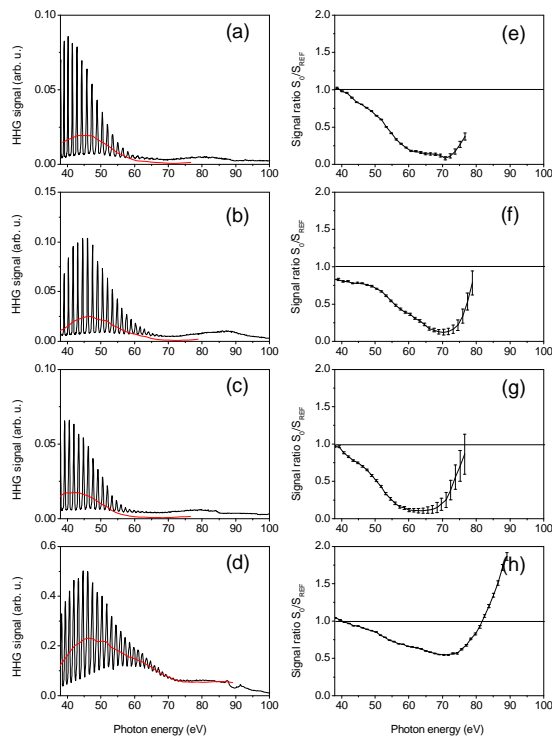


Figure 3. (a-d) HHG spectra of aligned CO_2 using a single-colour field of 1700, 1750, 1800, and 1850 nm. The red lines are the smoothed spectra used for the signal ratios. (e-h) Ratios between smoothed single-colour harmonic spectra of aligned (parallel to the driving field) and non-aligned CO_2 .

The ratios between spectra of aligned and nonaligned CO_2 molecules taken with different wavelengths of the driving field show a minimum whose position shifts from 64 eV to 72 eV. This shift could be a signature of hole dynamics in the molecule after ionisation [7,13].

Figure 4 shows the HHG spectra in non-aligned ethylene obtained with different wavelengths. A remarkable spectrum can still be observed with a driving field of 2000 nm. However, the extension of the cut-off, noticeable between 1650 nm and 1800 nm could not be taken much further due to the decrease of the laser energy available at longer wavelengths.

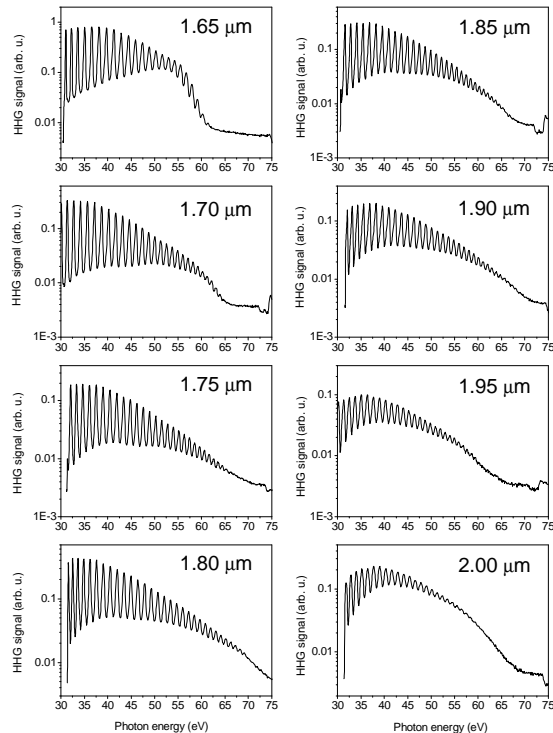


Figure 4. HHG of non-aligned ethylene in single-colour fields.

Conclusions

We have demonstrated the possibility to obtain HHG spectra with two-colour fields in aligned molecules and we have found that a single-colour field is sufficient to produce intense spectra even with wavelengths up to 2000 nm. However, the low laser energy available at these wavelengths prevents a dramatic cut-off extension. Therefore, the limiting factor for HHG spectroscopy with mid-IR fields is not the signal level but still the low harmonic cut-offs caused by the low laser energy.

Acknowledgements

This work has been funded through LASERLAB-EUROPE II (grant agreement no. 228334, EC's 7th Framework Programme).

References

1. M. Lein, J. Phys. B 40, R135–R173 (2007).
2. J. Marangos et al., Phys. Chem. Chem. Phys. 10, 35 (2008).
3. F. Krausz and M. Ivanov, Rev. Mod. Phys. 81,163 (2009).
4. R. Torres et al., Phys. Rev. Lett. 98, 203007 (2007).
5. N. Kajumba et al., New J. Phys. 10, 025008 (2008).
6. R. Torres et al., Opt. Exp. 18, 3174–3180 (2010).
7. R. Torres et al., Phys. Rev. A 81, 051802(R) (2010).
8. C. Vozzi et al., Appl. Phys. Lett. 97, 241103 (2010).
9. A. D. Shiner et al., Nat. Phys. 7, 464 (2011).
10. J. Tate et al., Phys. Rev. Lett. 98, 013901 (2007).
11. L. Chipperfield et al., Phys. Rev. Lett. 102, 063003 (2009).
12. T. Siegel et al., Opt. Exp. 18, 6853–6862 (2010).
13. O. Smirnova et al., Nature 460, 972 (2009).